JOURNAL OF GEOPHYSICAL RESEARCH, VOL. 107, NO. B12, 2370, doi:10.1029/2001JB000886, 2002

Thermal models of the Mexico subduction zone: Implications for the megathrust seismogenic zone

C. A. Currie[1]
School of Earth and Ocean Sciences, University of Victoria, Victoria, British Columbia, Canada

R. D. Hyndman[2] and K. Wang[2]
Pacific Geoscience Centre, Geological Survey of Canada, Sidney, British Columbia, Canada

V. Kostoglodov
Instituto de Geofisica, Universidad Nacional Autonoma de Mexico, Mexico City, Mexico

Received 2 August 2001; revised 8 August 2002; accepted 23 September 2002; published 26 December 2002.

[1] It has been proposed that the seismogenic zone of subduction thrust faults is primarily controlled by temperature or rock composition changes. We have developed numerical models of the thermal structure of the Mexico subduction zone to examine the factors that affect the temperature of the subduction thrust fault. Although the oceanic plates subducting beneath Mexico are young, the top of the oceanic plate at the trench is cool, because of the lack of a thick cover of insulating sediments. Marine heat flow observations suggest that hydrothermal circulation may further cool the oceanic plate. This results in a cool subduction thrust fault, where the brittle part of the fault extends to depths of over 40 km. At these depths, even slight frictional heating may have significant effects on temperature along the thrust fault, particularly for regions with a high convergence rate and shallow plate dip. With the addition of a small amount of frictional heating, the temperatures of the deep (30–40 km) thrust fault are increased by over 200°C. As the observed downdip limit of rupture in recent well-constrained megathrust earthquakes is confined to depths above the intersection of the thrust fault and the continental Moho, a temperature of 350°C may control the downdip extent of the seismogenic zone. Thus, in order to be consistent with the observed shallow rupture areas, it is necessary to include a small amount of frictional heating, corresponding to an average shear stress of 15 MPa. *INDEX TERMS:* 3015 Marine Geology and Geophysics: Heat flow (benthic) and hydrothermal processes; 3040 Marine Geology and Geophysics: Plate tectonics (8150, 8155, 8157, 8158); 7230 Seismology: Seismicity and seismotectonics; 8130 Tectonophysics: Evolution of the Earth: Heat generation and transport; *KEYWORDS:* thermal models, subduction zone, megathrust earthquakes, seismogenic zone, heat flow, Mexico subduction zone

Citation: Currie, C. A., R. D. Hyndman, K. Wang, and V. Kostoglodov, Thermal models of the Mexico subduction zone: Implications for the megathrust seismogenic zone, *J. Geophys. Res.*, *107*(B12), 2370, doi:10.1029/2001JB000886, 2002.

1. Introduction

[2] The Mexico subduction zone has experienced numerous megathrust earthquakes over the last century. Some of the largest earthquakes in recent history are the 1985 M_W 8.1 Michoacan earthquake and the 1995 M_W 8.0 earthquake in the Jalisco region. Such earthquakes pose a significant seismic hazard to the coastal regions of Mexico, as well as areas considerably inland, including Mexico City.

[3] Of particular importance to seismic hazard studies are the seaward (updip) and landward (downdip) limits of the seismogenic zone of the subduction thrust fault. These limits define the maximum earthquake rupture width, which is related to the maximum magnitude that may be expected for the fault. The downdip limit is the closest approach of the seismic source zone to cities, and thus is important for ground shaking hazard. The location of the updip limit is important for tsunami generation.

[4] It is hypothesized that temperature and rock composition provide the primary controls on the width and location of the seismogenic zone [e.g., *Zhang and Schwartz*, 1992; *Tichelaar and Ruff*, 1993; *Hyndman and Wang*, 1993; *Hyndman et al.*, 1997; *Peacock and Hyndman*, 1999]. In this study, we have developed thermal models of the Mexico subduction zone. We examine the factors that influence the temperature along the subduction thrust fault

[1]Also at Pacific Geoscience Centre, Geological Survey of Canada, Sidney, British Columbia, Canada.
[2]Also at School of Earth and Ocean Sciences, University of Victoria, Victoria, British Columbia, Canada.

0148-0227/02/2001JB000886$09.00

and then compare the thermal models to the observed rupture areas of recent megathrust earthquakes.

2. Constraints on Megathrust Earthquake Rupture Widths

[5] Globally, it is observed that only a shallow portion of the subduction fault is seismogenic [e.g., *Zhang and Schwartz*, 1992; *Tichelaar and Ruff*, 1993]. The seismogenic zone is bounded at its updip and downdip limits by regions that exhibit stable (aseismic) sliding (Figure 1). The transition from stable sliding to stick slip marks a change in fault behavior from velocity strengthening to velocity weakening [e.g., *Scholz*, 1990]. Although a number of factors may control fault behavior, we focus on temperature and composition.

2.1. Temperature Limits on Seismogenic Zone

[6] The presence of an updip aseismic zone has been attributed to the presence of stable sliding sediments [*Byrne et al.*, 1988; *Vrolijk*, 1990]. There are many factors that affect sediment properties, including pore fluid pressure and physical and chemical changes in the sediments [e.g., *Moore and Saffer*, 2001]. One change that may be important is the dehydration of smectite clays to illite and chlorite at temperatures between 100 and 150°C [*Wang*, 1980]. Whether this change marks the updip limit of the seismogenic zone remains a question [*Marone et al.*, 2001], and the thermal control on the frictional behavior of sediments along the subduction fault is a subject of active research.

[7] The downdip limit of the seismogenic zone is proposed to be limited by a temperature of 350°C for some subduction zones. Laboratory experiments show that quartzo-feldspathic continental rocks exhibit a transition from velocity weakening to velocity strengthening at temperatures of 325–350°C [*Tse and Rice*, 1986; *Blanpied et al.*, 1995]. This temperature agrees well with the maximum depth of earthquakes within continental crust [*Brace and Byerlee*, 1970; *Chen and Molnar*, 1983; *Tse and Rice*, 1986]. There may be a second temperature which limits the maximum rupture depth of megathrust earthquakes, initiated at temperatures less than 350°C. This second limit is proposed to be at about 450°C [*Hyndman and Wang*, 1993], corresponding to a rapid increase of instantaneous frictional stress in laboratory data [*Tse and Rice*, 1986].

[8] For southwest Japan, *Hyndman et al.* [1995] showed that the proposed thermal limits are consistent with both the coseismic rupture width and the seismogenic zone determined through modeling of coseismic and interseismic crustal deformation. For the Cascadia subduction zone, the proposed downdip thermal limit is consistent with interseismic geodetic observations [*Hyndman and Wang*, 1993; *Dragert et al.*, 1994; *Wang et al.*, 2003]. Both southwest Japan and Cascadia have young subducting plates.

2.2. Alternative Downdip Limit: Serpentinized Forearc Mantle Wedge

[9] For subduction zones with older subducting plates, such as Chile and south Alaska, *Oleskevich et al.* [1999] showed that the critical maximum temperatures are reached at depths greater than the intersection of the thrust fault with the continental Moho, whereas the maximum depth of rupture is limited to depths of 40–50 km [*Tichelaar and Ruff*, 1993]. These depths correspond to the depth of the continental Moho, and thus are consistent with the hypothesis that the intersection of the continental Moho and thrust fault provides the maximum downdip limit to the seismogenic zone [*Ruff and Tichelaar*, 1996]. One possible mechanism for generating stable sliding behavior of the fault below the continental Moho intersection is serpentinization of the mantle wedge. Dehydration reactions within the subducting plate release water into the overlying forearc mantle wedge, resulting in the formation of serpentine minerals and possibly other hydrous minerals, such as talc and brucite [*Peacock and Hyndman*, 1999]. Laboratory studies indicate that serpentinite generally exhibits stable sliding behavior [e.g., *Reinen*, 2000]. Although there are no laboratory studies of the sliding behavior of talc and brucite, their layered structure suggests that they are probably weak and aseismic. The existence of serpentine within the mantle wedge is supported by thermal and petrologic models [e.g., *Peacock*, 1993], as well as a number of seismological observations [e.g., *Suyehiro et al.*, 1996; *Kamiya and Kobayashi*, 2000; *Bostock et al.*, 2002].

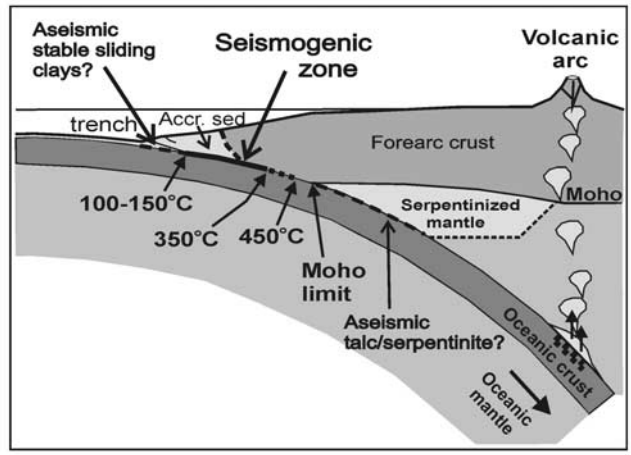

Figure 1. The proposed limits on the seismogenic zone of subduction thrust faults [after *Hyndman et al.*, 1997].

3. Thermal Modeling of the Mexico Subduction Zone

3.1. Numerical Approach

[10] In this study, the proposed controls on the megathrust seismogenic zone are examined through thermal modeling of the Mexico subduction zone, from the northern Rivera plate (~22°N) to the Tehuantepec Ridge on the Cocos plate (~15°N) (Figure 2). We have developed models for four profiles oriented perpendicular to the Middle America Trench. For each profile, a two-dimensional, steady state thermal model has been developed using the finite element approach described by *Wang et al.* [1995b]. We have also included subduction-induced mantle wedge flow, following *Peacock and Wang* [1999]. The thermal effects of mantle wedge flow on the shallow thrust fault are very small. The thrust temperature is increased by a maximum of 6°C at 40 km depth with the introduction of the flow.

[11] The critical parameters for thermal modeling are the geometry and age of the oceanic plate, the thickness and

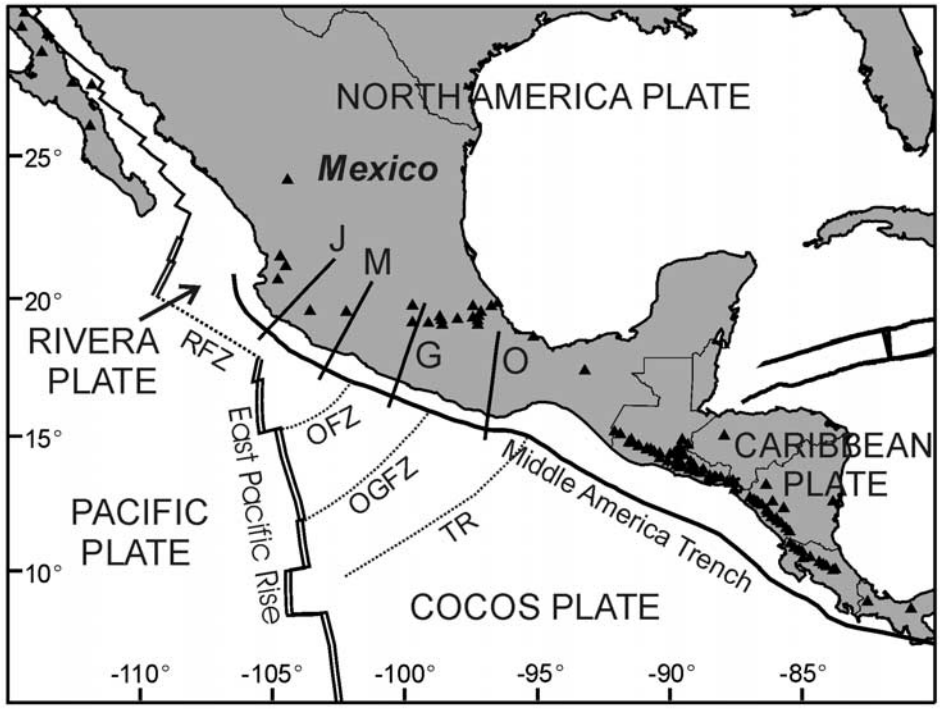

Figure 2. Tectonic map of Central America, showing the location of model cross sections: J, Jalisco; M, Michoacan; G, Guerrero; O, Oaxaca. Locations of active volcanoes are shown with triangles. The Trans-Mexico Volcanic Belt is located at ~20°N. Dotted lines are fracture zones: RFZ, Rivera Fracture Zone; OFZ, Orozco Fracture Zone; OGFZ, O'Gorman Fracture Zone; TR, Tehuantepec Ridge.

deposition history of incoming sediments, and the convergence rate. The thermal conductivity and radioactive heat generation of each rock unit must also be assigned. Two additional factors of potentially first-order importance are frictional heating along the thrust fault and hydrothermal circulation within the upper incoming oceanic crust.

[12] Also of potential importance is the thickness of the continental crust, as this defines the approximate location of the Moho intersection with the thrust fault. The crustal thickness beneath Mexico has been inferred from body and surface wave studies, seismic refraction surveys, and modeling of gravity and magnetotelluric data. In the northern part of the study region, *Gomberg et al.* [1989] and *Bandy et al.* [1999, and references therein] propose a crustal thickness of 36 to 40 km. To the south, crustal thickness studies give values of 33 km [*Couch and Woodcock*, 1981], 44 km [*Arzate et al.*, 1993], 45 ± 4 km [*Valdes et al.*, 1986], and 50 km [*Helsley et al.*, 1975]. In our modeling, we use a crustal thickness of 40 km for all profiles.

[13] The upper boundary of the model has a fixed temperature of 0°C. The base of the model is assigned a temperature of 1450°C, which approximates the mantle temperature at a depth of ~100 km. Because this boundary is located far from the region of interest (shallow subduction thrust fault) and because the primary control on the thermal regime is the seaward boundary condition, the basal boundary condition does not affect our results.

3.2. Oceanic Geotherm

[14] The seaward boundary condition for the two-dimensional model is a one-dimensional geotherm for the oceanic plate. There are several factors that control the temperature-depth profile of an oceanic plate: (1) conductive cooling of the plate as it ages, (2) the deposition of lower conductivity sediments on top of the plate that slow the rate of cooling, (3) the increase in sediment thickness over time, resulting in a colder sediment column, (4) compaction of sediments with increasing sedimentation, resulting in the expulsion of pore water, causing advective heat transfer within the sediments, and (5) hydrothermal circulation in the upper oceanic crust. In the following, we neglect the effects of hydrothermal circulation.

[15] The Rivera and Cocos plates are both young oceanic plates. Magnetic anomaly lineations [*Klitgord and Mammerickx*, 1982] indicate a slight increase in plate age to the southeast, from 11.5 Ma at the Jalisco profile to 15.5 Ma at the Oaxaca profile (Table 1). Multichannel seismic reflection data show that the northern Cocos plate and the Rivera plate are covered with no more than 200 m of sediment [*Michaud et al.*, 2000]. Seaward of the trench, the Cocos plate between the Guerrero and Oaxaca cross sections is covered with 170–200 m of pelagic and hemipelagic sedi-

Table 1. Oceanic Plate Parameters

Profile	Plate Age at Trench, Ma	Margin-Normal Convergence Rate, mm yr^{-1}	Plate Dip at 15 km Depth, deg
Jalisco	11.5	38	17.0
Michoacan	13.3	55	15.3
Guerrero A	13.1	58	15.3
Guerrero B	13.1	58	13.1
Oaxaca	15.5	61	11.3

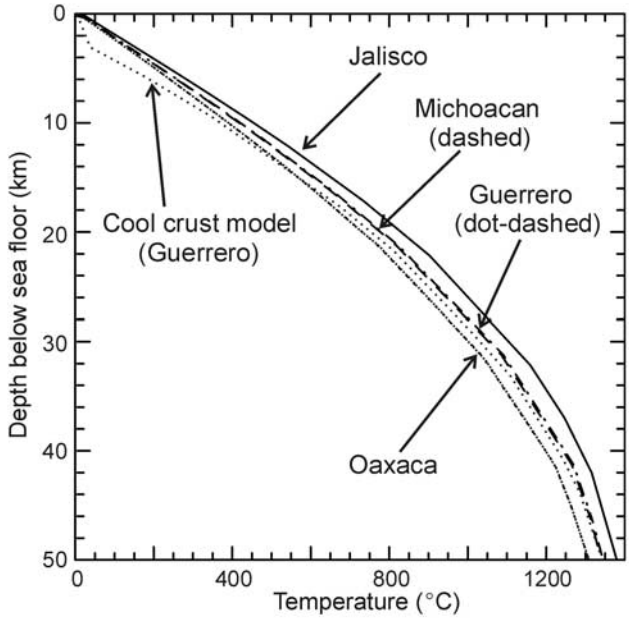

Figure 3. Oceanic geotherms for each profile. Also shown is the geotherm for the ''cool crust'' model for the Guerrero profile that approximates the effects of hydrothermal circulation to a depth of 3 km, using a plate age of 13.1 Ma.

ments [*Moore et al.*, 1982]. A uniform sediment thickness of 200 m on the incoming oceanic plate was used for all model profiles. Sediment deposition has occurred at a rate of 135 m Myr^{-1} over the last 0.78 Ma, and at a rate of 3–30 m Myr^{-1} before that [*Shephard and McMillen*, 1981]. Because of the small sediment thickness, uncertainties in the thickness and deposition rate have little effect on the oceanic crust thermal structure.

[16] Following the approach of *Wang and Davis* [1992], the oceanic geotherm can be calculated by allowing the plate to cool from zero years to its age at the trench, using the time-dependent sedimentation history and assuming a constant porosity-depth profile of the sediment column [*Hutchison*, 1985]. The resulting oceanic geotherms for each profile are shown on Figure 3. The Oaxaca geotherm has a slightly shallower gradient, due to the greater plate age. Despite the young age of the oceanic plates, the Mexico subduction zone is fairly cool relative to the Cascadia and southwest Japan subduction zones, which are of similar age [e.g., *Wang et al.*, 1995a, 1995b]. However, the oceanic plates in both of these regions are covered with 1.5 to 3.5 km of sediment, compared to ~200 m for the Mexico margin. The insulating effect of the thicker sediments results in a warmer subducting plate. At the trench, the temperature of the top of the oceanic plate is more than 200°C for the Cascadia subduction zone [e.g., *Hyndman and Wang*, 1993], whereas the temperature is 30 to 50°C for Mexico. The major uncertainty in the oceanic geotherms is the possible cooling of the upper oceanic plate by hydrothermal circulation (see discussion below).

3.3. Oceanic Plate Geometry

[17] For each profile, the geometry of the oceanic plate was defined using (1) single-channel and multichannel seismic reflection data, (2) seismic refraction data, (3) Wadati-Benioff earthquakes (assumed to occur about 5 km below the top of the oceanic plate), (4) intermediate magnitude thrust earthquakes, and (5) large megathrust earthquakes and their aftershocks. Data within 50 km of each profile were projected onto the cross section, and a best fit line was determined using a low-order polynomial (Figure 4). This geometry is similar to that given by *Pardo and Suarez* [1993, 1995]. The Jalisco profile also agrees well with the crustal structure determined through gravity modeling [*Bandy et al.*, 1999]. Estimated uncertainties in plate depth are 10%.

[18] Between the Orozco and O'Gorman Fracture Zones, it has been proposed that the Cocos plate flattens for a distance of 125 km at ~50 km depth [e.g., *Suarez et al.*, 1990; *Kostoglodov et al.*, 1996]. A line containing a subhorizontal section was fit to the data (Figure 4). A second geometry was determined using a smooth downward curvature, more consistent with the plate profiles to the north and south. Both profiles have a similar shape in the upper 30 km. The resulting thermal models show that the shallow thermal structure (<30–40 km depth) is not affected by the

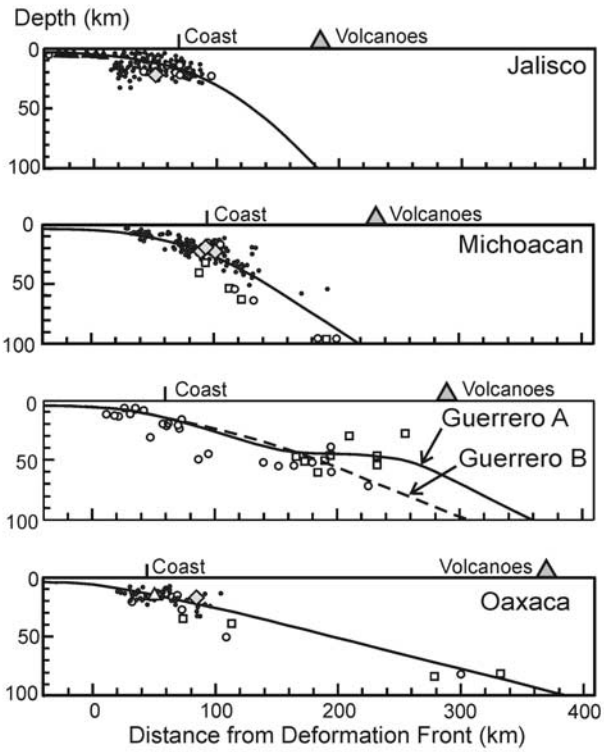

Figure 4. Geometry of subduction thrust fault along each profile. Open squares are in-slab earthquakes [*Singh et al.*, 2000]; open circles are relocated earthquakes [*Pardo and Suarez*, 1995]; solid triangles are seismic reflection data (Jalisco [*Michaud et al.*, 2000]); open triangle is from seismic refraction data (Oaxaca [*Nava et al.*, 1988]). Locations of megathrust main shocks (open diamonds) and their aftershocks (small circles) were given by *Pacheco et al.* [1997] for Jalisco], *Stolte et al.* [1986] for Michoacan, and *Singh et al.* [2000] for Oaxaca. Bathymetry data were used to constrain the plate surface seaward of the trench [*Prol-Ledesma et al.*, 1989; *Pardo and Suarez*, 1995].

presence or absence of the subhorizontal region, as the thermal structure is most sensitive to the shallow curvature (Figure 5).

3.4. Convergence Rate

[19] The convergence rate of the Cocos plate ranges from 5 cm yr^{-1} in the northwest to more than 7 cm yr^{-1} in the southeast [*DeMets and Wilson*,1997]. The margin-normal component of convergence is given in Table 1. The Rivera-North America convergence rate is much more controversial, with estimates ranging from 2 to 5 cm yr^{-1} [e.g., *Kostoglodov and Bandy*, 1995]. The most recent plate motion studies that use data from the last 0.78 Myr give convergence rates between 3.3 and 4.3 cm yr^{-1} along the Jalisco profile [*DeMets and Wilson*, 1997; *Bandy et al.*, 1998; *DeMets and Traylen*, 2000]. We use a steady state convergence velocity of 3.8 cm yr^{-1}. Variations of 0.5 cm yr^{-1} have little effect on the subduction thrust temperatures. *DeMets and Traylen* [2000] suggest that the convergence history of the Rivera plate is quite complex and variable over the past 10 Myr. On the basis of magnetic lineations, they propose the cessation or near cessation of convergence between 2.6 and 1.0 Ma. We have generated time-dependent thermal models containing the convergence history of *DeMets and Traylen* [2000]. The effect on the present thermal structure is minimal, and therefore the model results are not presented here. If a 1.6 Myr hiatus in subduction is introduced, the temperature of the top of the subducting plate increases slightly, and the locations of the 350 and 450°C isotherms are shifted ~7 km seaward of their steady state positions.

3.5. Thermal Parameters

[20] Each of the two-dimensional models has four units: oceanic plate, sediments, continental crust, and mantle wedge. The thermal conductivity of the entire continental crust is taken as 2.5 W m^{-1} K^{-1}. This is a reasonable value for continental crust material [e.g., *Peacock and Wang*, 1999] and is consistent with that measured during continental heat flow studies of Mexico [*Smith et al.*, 1979; *Ziagos et al.*, 1985]. Although there may be localized regions of the crust with varying conductivity, it is only the large-scale crustal conductivity that is of importance in the current study. The upper 15 km of the continental crust is assigned a radioactive heat generation of 1.3 μW m^{-3}, while the lower 25 km is 0.27 μW m^{-3}. These are typical continental values and reflect the roughly exponential decrease in radioactive heat production with depth (e.g., discussion by *Peacock and Wang* [1999]). These values are also comparable with measurements by *Ziagos et al.* [1985] which gave values of 1.3 ± 0.6 μW m^{-3} for the upper 4 km. Variation in continental heat generation by a factor of two has a minimal effect on the temperature of the thrust fault but significantly affects surface heat flow (Figure 5).

[21] The accretionary prism and sediments have conductivities that increase landward and with depth from 1.0 W m^{-1} K^{-1} at the seafloor to 2.0 W m^{-1} K^{-1} at 10 km depth. The seafloor value is consistent with marine heat flow measurements in this area [e.g., *Vacquier et al.*, 1967; *Prol-Ledesma et al.*, 1989]. A uniform volumetric heat production rate of 1.0 μW m^{-3} is assigned to the accretionary prism and sediments, which is similar to the average upper continental source rock for the sediments.

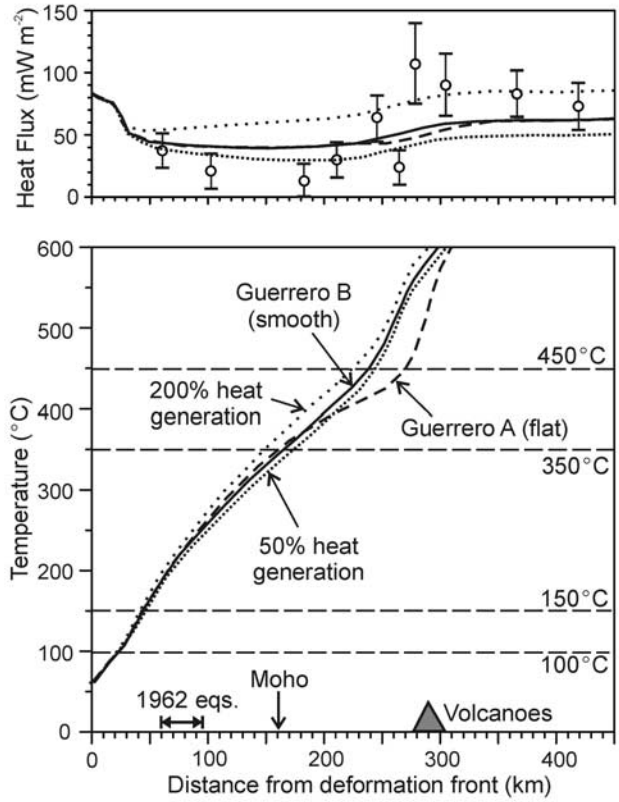

Figure 5. Variations in (top) surface heat flow and (bottom) temperatures on the top of the oceanic plate for various models along the Guerrero profile. The effects of plate dip profile and amount of continental heat generation are investigated. None of the models contain frictional heating or hydrothermal circulation. Heat flow measurements are from *Ziagos et al.* [1985].

[22] Parameter values for the mantle wedge and oceanic plate are those used in previous modeling studies [e.g., *Hyndman and Wang*, 1993, 1995; *Oleskevich et al.*, 1999]. A conductivity of 2.9 and 3.1 W m^{-1} K^{-1} is assigned to the oceanic plate and mantle, respectively. Both units have a radioactive heat generation of 0.02 μW m^{-3} and a volumetric heat capacity of 3.3 MJ m^{-3} K^{-1}. Reasonable variations in these values have only a small effect on the thermal structure [e.g., *Wang et al.*, 1995a].

3.6. Frictional Heating

[23] The temperature of the thrust fault may be affected by frictional heating [e.g., *van den Beukel and Wortel*, 1987; *Molnar and England*, 1990; *Dimitru*, 1991]. Following the procedure of *van den Beukel and Wortel* [1987] and *Wang et al.* [1995a, 1995b], frictional heating is incorporated into the thermal models by dividing the fault interface into two zones: a shallow region of brittle frictional sliding and a deeper region of ductile shear. In the brittle region, the shear stress along the fault is given by Byerlee's law of friction [*Byerlee*, 1978]. The shear stress increases with depth, due to the increase in normal stress, approximated by the load of the overlying rock column. The pore pressure ratio is assumed to be constant with depth. A decrease in the pore pressure ratio corresponds to an increase in frictional heat-

ing. In the deeper plastic regime, the magnitude of heating is given by the viscous stress along the fault, determined from the strain rate using the power law rheology for diabase [e.g., *Caristan*, 1982]. In this region, the magnitude of shear stress decreases with depth, due to increasing temperature. Thus the maximum shear stress is found at the transition between brittle and ductile behavior. The transition from brittle sliding to ductile shear is temperature-dependent, and thus, an iterative approach was used in the modeling, following *Wang et al.* [1995b]. Frictional heating was introduced to a maximum depth of 40 km. Below this, the fault interface is inferred to be in contact with the serpentinized mantle wedge, which is believed to be too weak to allow significant frictional heating.

[24] As the incoming oceanic crust at the Mexico subduction zone is cool, the brittle-ductile transition along the subduction thrust fault occurs at depths >30 km, and frictional heating may not be negligible. We have tested the effects of varying amounts of frictional heating on the thrust fault. Decreasing the pore pressure ratio from 1.0 (no frictional heating) to 0.9 corresponds to an increase in average shear stress along the fault from 0 to 31 MPa, or an effective coefficient of friction (defined by the ratio of the shear to normal stresses along the fault) from 0 to 0.068. These are within the ranges determined in previous studies of subduction thrust faults [e.g., *van den Beukel and Wortel*, 1987; *Wang et al.*, 1995a, 1995b; *Wang and He*, 1999]. Figure 6 illustrates the effects of frictional heating on the temperatures of the top of the subducting plate. The large peak in the temperature profile near the Moho intersection is a result of the termination of frictional heating at this depth.

[25] The effect of frictional heating at shallow depths (<20 km) is quite small. With a pore pressure ratio of 0.9, the 100°C and 150°C isotherms are shifted a maximum of 10 km seaward from models without frictional heating. The inclusion of the maximum amount of frictional heating results in a seaward shift of the 350°C isotherm of 23 km (Jalisco) to 89 km (Oaxaca) from its position in models with no frictional heating. The position of the 450°C isotherm is shifted seaward by 30 km (Jalisco) to 170 km (Oaxaca). Frictional heating has the largest effect for profiles with a high convergence rate and shallow plate dip (e.g., the Oaxaca profile). At 40 km depth, the thrust fault along the Oaxaca profile is 200°C warmer with the addition of frictional heating, compared to an increase of ~120°C for Jalisco.

3.7. Hydrothermal Circulation

[26] An additional uncertainty in the shallow thrust temperatures comes from possible hydrothermal circulation within the upper oceanic plate. Marine heat flow studies have shown that the heat flow near the trench offshore Mexico is lower than that predicted for a cooling oceanic plate overlain by sediments (Figure 6). This suggests that hydrothermal circulation in the upper oceanic crust may occur in this region. This mechanism has been used to explain the anomalously low heat flow values observed offshore Costa Rica [*Langseth and Silver*, 1996; *Harris and Wang*, 2002].

[27] We developed a ''cool crust'' thermal model to approximate the effects of hydrothermal circulation for all profiles, using the method of *Langseth and Silver* [1996] and *Harris and Wang* [2002]. In the model, the oceanic geotherm was designed to contain a 3 km thick convectively cooled layer that produces a surface heat flow of 30 mW m^{-2}, consistent with the observations (Figure 3). This model examines the maximum thermal effects on the shallow thrust fault and may not accurately model the deep temperatures. The effect on the surface heat flow is confined to the regions near the deformation front (Figure 6). At distances >100 km, the resulting surface heat flow is indistinguishable from the original models. With hydrothermal cooling to a depth of 3 km, the location of the 100°C and 150°C isotherms are shifted ~10 km landward. For hydrothermal cooling to depths <3 km, the landward shift is less.

3.8. Uncertainties in the Thermal Models

[28] Figure 6 illustrates the range of temperatures along the top of the subducting plate from our modeling, for variations in frictional heating (pore pressure ratio of 1.0–0.9) and the inclusion of hydrothermal circulation. The amount of frictional heating provides the major uncertainty in the models, particularly the deep (>20 km) temperatures.

[29] For each of the models shown in Figure 6, an additional uncertainty comes from the other modeling parameters. In western Mexico, the age of the oceanic plate, the incoming sediment thickness and convergence rate are relatively well constrained. The subducting plate profile remains fairly uncertain, particularly at depths greater than 30–40 km. However, a variation in plate dip by more than 20% is required to produce significant changes in the temperature of the top of the oceanic plate. This is much greater than the estimated uncertainty of 10% in the shallow plate profile. While the values of the thermal parameters (thermal conductivity and radioactive heat production) are relatively uncertain for the continental crust, these parameters have little effect on the temperature of the plate interface. A reasonable variation of 0.5 W m^{-1} K^{-1} of the thermal conductivity of the entire continental crust and accretionary prism results in a change in thrust temperature of <15°C. Radioactive heat production in the continental crust significantly affects the surface heat flux, but only has a small effect on the plate surface temperature (Figure 5). We estimate that these factors result in an additional uncertainty in the position of the 100°C isotherm of 15 km. The additional uncertainty in the location of the 350°C and 450°C isotherms is 20 km.

4. Surface Heat Flux Observations

[30] An independent constraint on the thermal models is surface heat flux observations (Figures 5 and 6). Low values of heat flow observed near the trench on the Michoacan and Oaxaca profiles are better fit by models containing hydrothermal circulation. For all models, the forearc has a modeled heat flux of 40–50 mW m^{-2} (Figure 6), which is slightly larger than most of the borehole heat flow measurements by *Ziagos et al.* [1985]. The surface heat flow is highly dependent on the amount of radioactive heat generation in the continental crust. By reducing the crustal heat generation, the modeled values will better fit the observations (Figure 5).

[31] However, the observed heat flux values have large uncertainties. The boreholes used were very shallow (many were <200 m depth). Few thermal conductivity measurements were taken for each hole, and steep topography at many sites required a terrain correction to the data, further increasing the uncertainty. In addition, the complex geo-

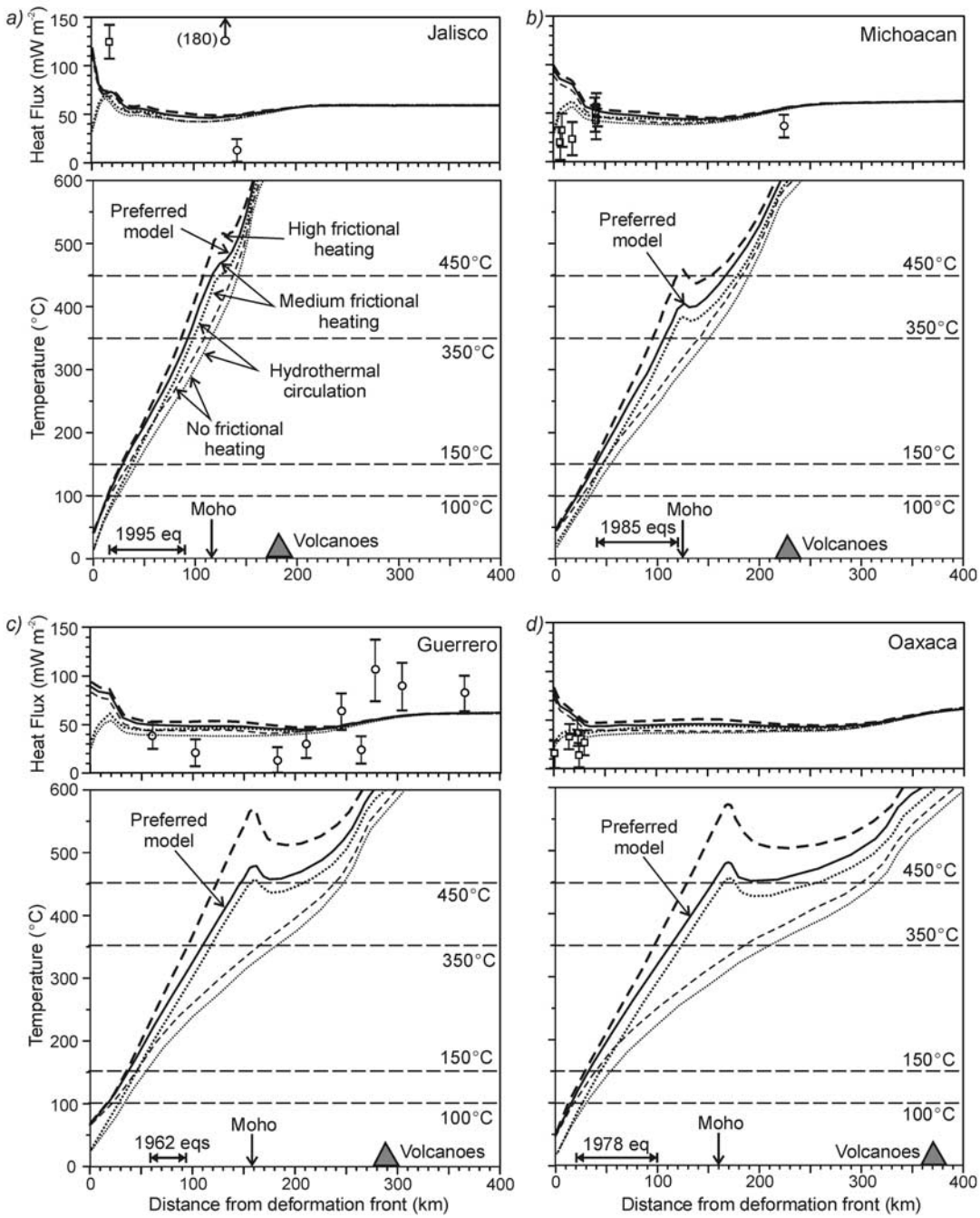

Figure 6. Variations in (top) surface heat flow and (bottom) temperatures on the top of the oceanic plate for varying amounts of frictional heating. The thin dashed line indicates a model with no frictional heating; the solid line is a model which uses a pore pressure ratio of 0.94 (medium frictional heating); the thick dashed line is a high frictional heating model, using a pore pressure ratio of 0.90. The introduction of frictional heating causes the peak in the temperature profile near the Moho intersection, as heating was introduced only to this depth. Dotted lines indicate the results for models with hydrothermal circulation to a depth of 3 km within the incoming oceanic plate (thin dotted line is a model with no frictional heating; thicker dotted line is a model with medium frictional heating). For models with hydrothermal circulation to depths <3 km, the effects on thrust temperature are smaller. The rupture widths of past earthquakes are indicated. The Guerrero profile uses the Guerrero B geometry. Heat flow measurements are from *Ziagos et al.* [1985] (circles) and *Prol-Ledesma et al.* [1989] (squares).

logical setting of Mexico results in small-scale lateral variations in surface heat flow due to local geological or hydrogeological effects [*Prol-Ledesma*, 1991]. For example, in the forearc near the Jalisco profile, heat flow values of 13 and 180 mW m^{-2} were recorded within 200 km of each other [*Ziagos et al.*, 1985]. On the basis of these factors, we have assigned an uncertainty of 20% to each heat flow observation. The introduction of frictional heating results in a surface heat flow increase of <10 mW m^{-2} (Figure 6). Given the present quality of forearc heat flow data and uncertain radioactive heat generation, the existing data cannot constrain the magnitude of frictional heating. The observations suggest that frictional heating must be small but do not exclude it. Future continental heat flux and radioactive heat generation studies in Mexico to constrain thrust temperatures should focus on the continental shelf and coastal areas, as these regions are most sensitive to frictional heating along the fault.

[32] With the simple model of mantle wedge circulation, an increase in heat flux is observed near the volcanic arc (Figure 5 and 6). This is consistent with the increase in heat flow documented by *Ziagos et al.* [1985] over the Trans-Mexico Volcanic Belt. However, the sharp increase from the forearc to the back arc is not reproduced by our model. This sharp transition is likely due to near-surface processes associated with volcanism, such as a magma emplacement, which are not included in our models. Our modeled back arc heat flow is consistently lower than the observed values. Heat flow in the back arc is the result of a number of complex processes, including mantle wedge circulation, and magma generation and emplacement. The effects of such processes on the seismogenic zone (>150 km away) are small.

5. Mexico Seismogenic Zone

5.1. Past Megathrust Earthquakes

[33] The thermal models can be compared to the rupture widths of past megathrust earthquakes to investigate possible thermal controls on the seismogenic zone. Below, we summarize well-studied earthquakes for each profile.

5.1.1. Jalisco

[34] On 3 and 18 June 1932, two earthquakes occurred north of the proposed Rivera-Cocos plate boundary (M_S 8.2 and 7.8, respectively). Aftershocks from these earthquakes have a seaward limit 10–15 km from the trench and extend to 90–95 km from the trench [*Singh et al.*, 1985]. In 1995, an M_W 8.0 earthquake occurred in the southern part of this region (Figure 7a). The majority of aftershocks for this earthquake were located between 20 and 100 km from the trench [*Pacheco et al.*, 1997]. As the aftershocks were located using a local station array and a local velocity model, we estimate the location uncertainty to be as small as ±5 km. The aftershock area is in good agreement with the results of waveform modeling that determined a nearly rectangular rupture area, oriented parallel to the Middle America trench, with a margin-normal width of 90 km [*Mendoza and Hartzell*, 1999].

[35] Geodetic observations provide additional constraints on the updip and downdip limits of rupture. Modeling of tsunami records from two local tide gauges indicates that the maximum seafloor uplift was located 24 ± 5 km from the trench [*Ortiz et al.*, 2000b]. The downdip limit was constrained through GPS observations from a dense GPS network located directly onshore. Both *Melbourne et al.* [1997] and *Hutton et al.* [2001] were able to fit GPS observations with heterogeneous coseismic slip along the thrust fault to a depth of ~23 km using an elastic model. This corresponds to a downdip limit located 90 km from the trench.

[36] Primarily using the relocated aftershocks for the 1995 earthquake [*Pacheco et al.*, 1997], we have taken the seismic rupture width in the Jalisco region to be 75 km, located between 15 and 90 km from the trench (Figure 7a). On the basis of the good agreement among the various types of observations, uncertainties in this width are small.

5.1.2. Michoacan

[37] On 19 September 1985, an M_W 8.1 earthquake occurred on the Michoacan segment of the Cocos-North America interface (Figure 7b). This was followed 2 days later by an M_W 7.7 earthquake to the southeast. The majority of aftershocks for both events were located between 40 and 120 km from the trench [*UNAM Seismology Group*, 1986; *Stolte et al.*, 1986]. The width of the aftershock area is slightly narrower in the northwest part of the 19 September rupture area, with the landward limit of the aftershocks ~80 km from the trench. Waveform inversion of the 19 September earthquake indicates that slip occurred between depths of 6 and 39 km [*Mendoza and Hartzell*, 1989], in good agreement with the aftershock rupture area. The locations of the updip and downdip limits of rupture from both types of studies are relatively well constrained due to a close station spacing and the use of a locally derived velocity model. There are no published tsunami models constraining the updip limit of rupture of the 19 September earthquake. However, distant stations recorded a tsunami with a very low amplitude, which suggests that rupture did not extend all the way to the seafloor [*UNAM Seismology Group*, 1986]. On the basis of the above studies, seismic rupture in the Michoacan region appears to have occurred between 40 and 120 km from the trench (Figure 7b).

5.1.3. Guerrero

[38] The region northwest of the Guerrero profile is referred to as the Guerrero gap as there have been no large megathrust earthquakes for at least 90 years [e.g., *Ortiz et al.*, 2000a]. However, southeast of the profile, there were two small thrust earthquakes in 1962 within eight days of each other, with magnitudes of 7.1 and 7.0. Southeast of these earthquakes, there was a magnitude 7.8 earthquake in 1957. Although the rupture area of these three earthquakes has been defined using the aftershock distribution (Figure 7c), this area has large uncertainties due to a poor regional station distribution [*Ortiz et al.*, 2000a]. Modeling of the tsunamis generated by these earthquakes has provided stronger constraints on the rupture area. The modeled updip limit of all three earthquakes is located at 60 ± 10 from the trench [*Ortiz et al.*, 2000a]. The width of the 1962 rupture area is 35 km, while the width of the 1957 earthquake may be as much as 70 km. Uncertainties in the downdip rupture limit are large, as this limit is not well constrained by tsunami observations.

5.1.4. Oaxaca

[39] The Oaxaca profile passes through the rupture area of the 1978 M_W 7.6 earthquake (Figure 7d). The 1-month aftershocks for this earthquake extend from 20 to 100 km from the trench [*Singh et al.*, 1980; *Stewart et al.*, 1981]. As

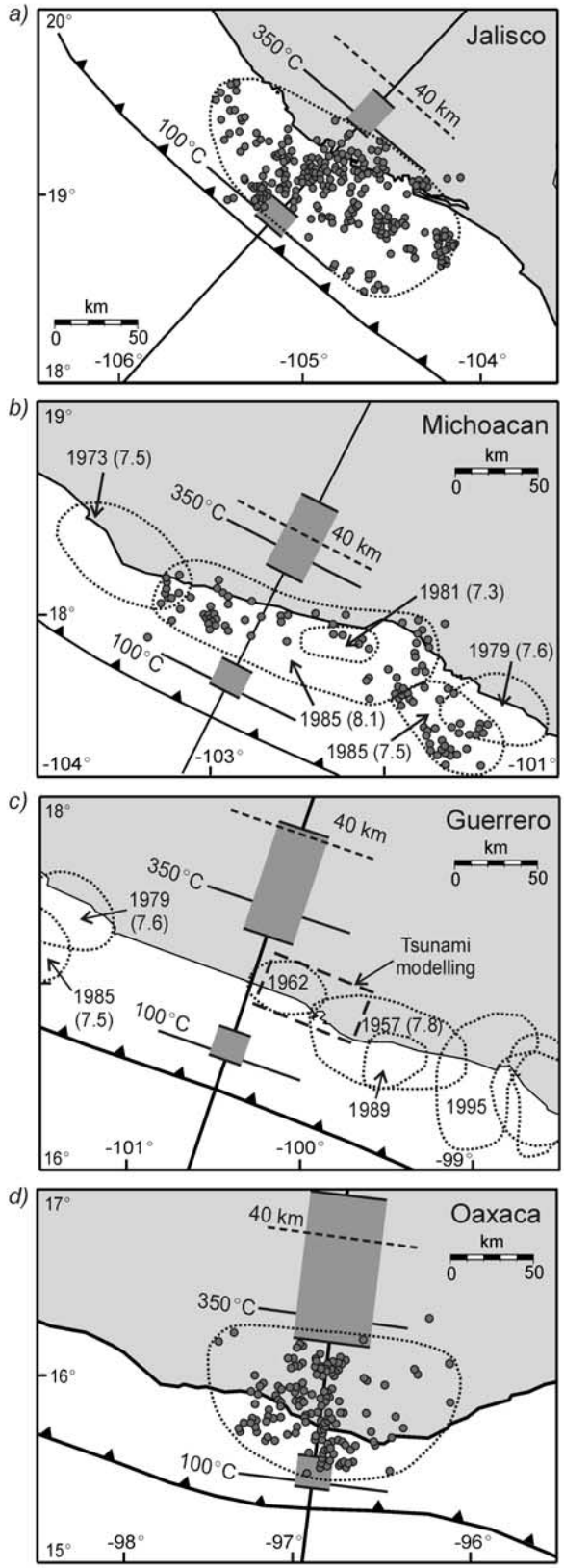

the aftershocks were located relative to the main shock, the relative positions of each earthquake are very well constrained. In addition, the aftershocks extend well under the coast and were recorded using a number of local portable seismic stations. Thus the uncertainties in the absolute lateral location of the group of aftershocks are likely less than ±5 km (J. Cassidy, personal communication, 2002).

5.2. Thrust Intersection With Mantle

[40] The observed rupture widths for megathrust earthquakes near each profile are shown on Figure 7. The intersection of the continental Moho with the subduction fault may mark the maximum downdip limit to the seismogenic zone. As discussed above, the continental crustal thickness is not well resolved for the Mexico margin. The Moho intersection with the subduction fault was taken to occur at a depth of 40 km. This corresponds to a lateral distance of 117 km between the Moho intersection and the trench on the Jalisco profile, increasing to 160 km on the Oaxaca profile, due to the shallower plate dip in the southeast. If the crust is as thin as 33 km, the Moho intersection will be shifted seaward by 15 km (Jalisco) to 25 km (Oaxaca). For a Moho at 50 km depth, the intersection with the fault will be shifted landward by 15–35 km. Thus, for all Moho depths the observed earthquake rupture areas in Jalisco, Guerrero and Oaxaca are updip of the intersection of the continental Moho with the thrust fault. In the middle of the 1985 Michoacan earthquake rupture area, observations suggest that rupture may have extended to the Moho. However, to the northwest and southeast, rupture was much narrower and significantly updip of the Moho intersection.

5.3. Comparison of Rupture Areas to Thermal Models

[41] A downdip change in properties along the thrust fault appears to limit the downdip extent of rupture to depths shallower than the Moho intersection. We focus on the hypothesis that thrust fault temperature provides the primary control on the sliding behavior of the fault. As discussed above, we take the 100 and 350°C isotherms as the thermal limits on the seismogenic zone of the thrust fault. Assuming that the proposed thermal limits are correct, it is necessary to introduce a small amount of frictional heating to the thermal models of Mexico to be consistent with the

Figure 7. (opposite) Comparison of the aftershock areas of recent megathrust earthquakes with the thermal model results. (a) The 11-day aftershocks for the 1995 Jalisco earthquake [*Pacheco et al.*, 1997]; (b) 11-day aftershocks for the 1985 Michoacan earthquakes [*UNAM Seismology Group*, 1986], also shown are rupture areas and magnitudes of past earthquakes in this region [after *Kostoglodov and Pacheco*, 1999]; (c) 1962 earthquake rupture limits from tsunami modeling [*Ortiz et al.*, 2000a] and from the poorly constrained aftershock distribution [*Kostoglodov and Pacheco*, 1999]; and (d) 33-day aftershocks for the 1978 Oaxaca earthquake [*Stewart et al.*, 1981]. The shaded bars represent the range in the position of the 100 and 350°C isotherms, based on the models shown in Figure 6. The solid line indicates the position of these isotherms for the preferred model. The Moho intersection at 40 km depth is also shown (dashed line).

observed shallow downdip rupture limit. For models with no frictional heating, the location of the 350°C isotherm is landward of the fault intersection with the Moho and much deeper than the observed rupture limit. If the alternative hypothesis that the Moho intersection provides the maximum downdip limit of the seismogenic zone is correct, the seismogenic zone width would be 100–145 km along the Mexican margin, significantly wider than the observed rupture widths.

[42] Thermal models that include a small amount of frictional heating, using a pore pressure ratio of 0.94, provide the best agreement with the observed earthquake rupture areas along the entire margin. This corresponds to an average shear stress of ~15 MPa, or an effective coefficient of friction of 0.041, consistent with estimates for other subduction faults [e.g., *van den Beukel and Wortel*, 1987; *Wang et al.*, 1995b; *Wang and He*, 1999]. It is also consistent with a previous thermal model for Mexico that concludes that frictional heating must be fairly small at shallow depths [*Ziagos et al.*, 1985]. Most subduction thrust faults are believed to be weak. *Wang et al.* [1995a, 1995b] assumed negligible frictional heating in Cascadia and southwest Japan thermal models. For these subduction zones, a pore pressure ratio of 0.94 leads to an average shear stress of <7 MPa because the brittle part of the fault is confined to depths <20 km. The thermal effect of this small shear stress is well within model uncertainties. Frictional heating was not included in the thermal models of the south Alaska and Chile subduction zones [*Oleskevich et al.*, 1999]. For south Alaska and Chile, even with frictional heating, the position of the 350°C isotherm is much deeper than the Moho intersection with the thrust fault, and therefore does not change their conclusion that the downdip limit of megathrust earthquakes in these regions may be limited by the Moho intersection.

[43] Figure 8 shows the thermal models for each profile, using a pore pressure ratio of 0.94. The temperature along the top of the oceanic plate at depths <20 km is similar for all profiles. The intersection of the 100°C isotherm occurs ~15–20 km landward of the trench. The intersection of the 350°C isotherm occurs 92 km from the trench on the Jalisco profile. It is further landward on the other profiles (~110 km). This is due to the younger age of subducting crust, the slower convergence rate, and the steeper plate dip of the Jalisco profile. The downdip transition zone is inferred to extend to the Moho intersection for all profiles. The Moho intersection coincides with a temperature of ~450°C along the Jalisco, Guerrero, and Oaxaca profiles. The temperature at the Moho intersection is ~400°C along the Michoacan profile. Using the proposed thermal limits on the seismogenic zone, the above thermal models give a seismogenic zone downdip width 80–100 km along the margin (Figure 9). There is a very good agreement between the well-constrained observed downdip limit of rupture and the proposed downdip temperature limit of 350°C in the Jalisco and Oaxaca regions. The agreement is poorer in the Michoacan and Guerrero regions. The majority of seismic rupture of the 1985 Michoacan earthquakes occurred further updip. The downdip limit of rupture in the Guerrero region is poorly constrained, but observations suggest that it was also significantly updip of the proposed thermal limit. The 1962 and 1957 earthquakes in the Guerrero region were quite small. As there are no large scale differences in the factors controlling the thermal regime between the four regions, it is possible that these earthquakes did not rupture the entire downdip width of the proposed thermally limited seismogenic zone.

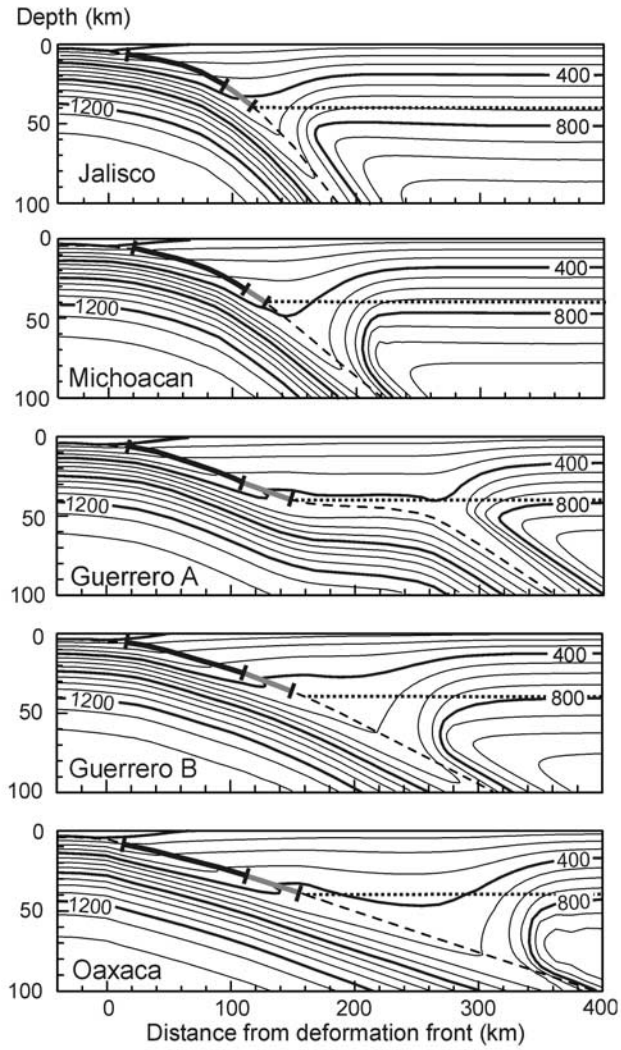

Figure 8. Preferred thermal models for each profile with 100°C isotherms. The dark line indicates the proposed thermally limited seismogenic zone; the gray line is the transition zone. The dashed line is the top of the oceanic plate, and the dotted line is the continental Moho.

[44] The shallow fault temperatures are relatively unaffected by frictional heating, and thus, in all models, the proposed updip limit of 100°C is in good agreement with the observed seaward limit of rupture for the 1995 Jalisco and 1978 Oaxaca earthquakes. The updip limit of rupture of the 1985 Michoacan earthquakes corresponds to a temperature of ~150°C. In the Guerrero region, the updip rupture limit of the 1962 earthquakes, as determined through tsunami modeling, is at a temperature of over 200°C. With the inclusion of hydrothermal cooling, the fault temperatures are decreased, and the observed updip rupture limits are more compatible with the proposed thermal limit (Figure 9). The good agreement of the observed updip limit of rupture for most of the megathrust earthquakes with the

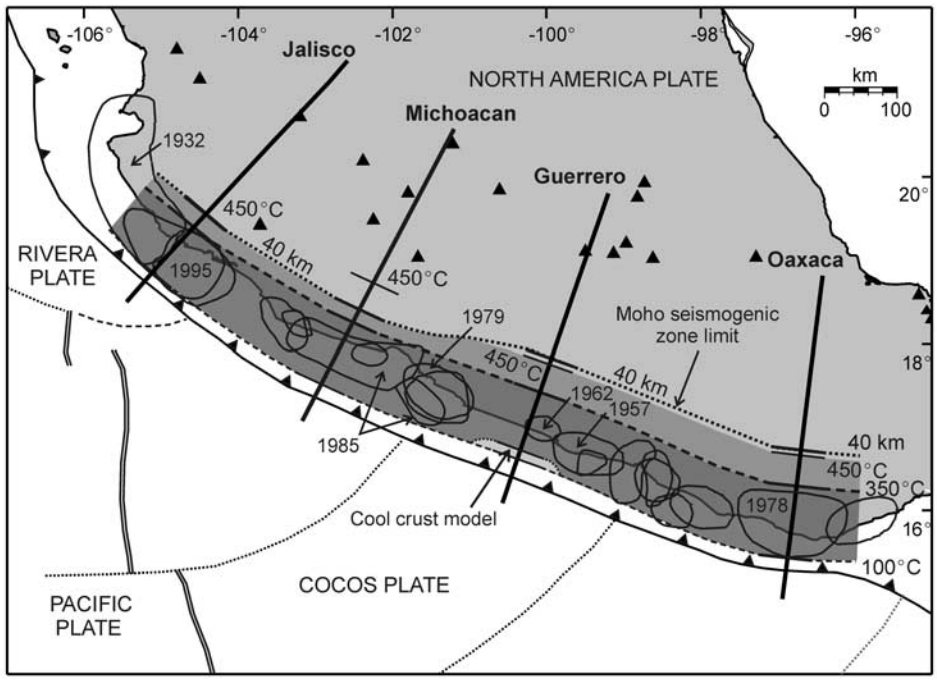

Figure 9. Map of proposed thermally defined seismogenic zone (darker shading). With no frictional heating, the seismogenic zone may be limited by the intersection of the thrust fault with the continental Moho (40 km depth). Also shown are the rupture areas of past megathrust earthquakes [modified from *Kostoglodov and Pacheco*, 1999]. Earthquakes discussed in text are labeled. The light region at the seaward end of the Guerrero profile indicates the landward shift in the 100°C isotherm for the model containing hydrothermal circulation.

proposed thermal limit of 100–150°C suggests that hydrothermal cooling is probably a local effect.

6. Conclusions

[45] We have developed two-dimensional, steady state thermal models for four cross sections through the Mexico subduction zone. Despite the young age of the subducting Rivera and Cocos plates, they are much cooler than oceanic plates in other warm slab subduction zones, such as Cascadia and southwest Japan. This is primarily due to only a thin cover of insulating sediments on the oceanic plates. The thin sediment cover may also allow hydrothermal circulation in the upper oceanic crust, resulting in an even cooler plate surface.

[46] Because of the cool subducting plate, the overall thermal structure of the Mexico subduction zone is intermediate between subduction zones with young, hot oceanic plates (e.g., Cascadia and southwest Japan) and those with older oceanic plates (e.g., south Alaska and Chile). The cool subducting plate surface means that the brittle part of the subducting plate surface extends to depths of 30–40 km. When brittle friction occurs at depths >20 km, even a very weak fault may produce significant frictional heating. Our results show that a small amount of frictional heating can have a large effect on the thrust temperatures. The deep (30–40 km) part of the thrust fault can be increased by over 200°C with the inclusion of only a small amount of frictional heating. The effect of frictional heating is largest for areas that have a shallowly dipping plate and a high convergence rate.

[47] For the Mexico subduction zone, megathrust earthquake rupture is confined to depths <30 km. If the downdip limit of rupture is controlled by a temperature of 350°C, a small amount of frictional heating must be included in the thermal models. The models that best fit the observed rupture along the entire margin use an average shear stress of 15 MPa, consistent with the conclusion of past studies of a weak subduction fault and low frictional heating. The observed updip limit of coseismic rupture, although poorly constrained, is in agreement with a thrust temperature of 100°C for much of the margin. For all models, the proposed downdip thermal limit of the seismogenic zone occurs landward of the coast, with a transition zone that extends up to 80 km inland. This is important for seismic hazard studies for Mexico, as the seismic source zone could underlie populated areas.

[48] **Acknowledgments.** We thank S. Mazzotti, S. Peacock, S. Schwartz, and an anonymous reviewer for their thoughtful reviews which improved the manuscript. We acknowledge helpful discussions with J. Cassidy, H. Dragert, W. Hutton, T. Lewis, G. Rogers, and S. Singh. Maps were generated using GMT software [*Wessell and Smith*, 1995]. Support for C. Currie provided by an NSERC graduate scholarship and the Canadian GEOIDE project. Research support provided by USGS NEHRP grants 00HQGR0061 and 01HQGR0058. Geological Survey of Canada contribution 2001086.

References

Arzate, J. A., M. Mareschal, and J. Urrutia-Fucugauchi, A preliminary crustal model of the Oaxaca continental margin and subduction zone from magnetotelluric and gravity measurements, *Geofis. Int.*, *32*, 441–452, 1993.

Bandy, W. L., V. Kostoglodov, and C. A. Mortera-Gutierrez, Southwest migration of the instantaneous Rivera-Pacific Euler pole since 0.78 Ma, *Geofis. Int.*, *37*, 153–169, 1998.

Bandy, W., V. Kostoglodov, A. Hurtado-Diaz, and M. Mena, Structure of the southern Jalisco subduction zone, Mexico, as inferred from gravity and seismicity, *Geofis. Int.*, *38*, 127–136, 1999.

Blanpied, M. L., D. A. Lockner, and J. D. Byerlee, Frictional slip of granite at hydrothermal conditions, *J. Geophys. Res.*, *100*, 13,045–13,064, 1995.

Bostock, M. G., R. D. Hyndman, S. Rondenay, and S. M. Peacock, An inverted continental Moho and serpentinization of the forearc mantle, *Nature*, *417*, 536–538, 2002.

Brace, W. F., and J. D. Byerlee, California earthquakes: Why only shallow focus?, *Science*, *168*, 1573–1575, 1970.

Byerlee, J. D., Friction of rocks, *Pure Appl. Geophys.*, *116*, 615–626, 1978.

Byrne, D. E., D. M. Davis, and L. R. Sykes, Loci and maximum size of thrust earthquakes and the mechanics of the shallow region of subduction zones, *Tectonics*, *7*, 833–857, 1988.

Caristan, Y., The transition from high temperature creep to fracture in Maryland diabase, *J. Geophys. Res.*, *87*, 6781–6790, 1982.

Chen, W., and P. Molnar, Focal depth of intracontinental and interplate earthquakes and its implications for the thermal and mechanical properties of the lithosphere, *J. Geophys. Res.*, *88*, 4183–4214, 1983.

Couch, R., and S. Woodcock, Gravity and structure of the continental margins of southwestern Mexico and northwestern Guatemala, *J. Geophys. Res.*, *86*, 1829–1840, 1981.

DeMets, C., and S. Traylen, Motion of the Rivera plate since 10 Ma relative to the Pacific and North American plates and the mantle, *Tectonophysics*, *318*, 119–159, 2000.

DeMets, C., and D. S. Wilson, Relative motions of the Pacific, Rivera, North American, and Cocos plates since 0.78 Ma, *J. Geophys. Res.*, *102*, 2789–2806, 1997.

Dimitru, T. A., Effect of subduction parameters on geothermal gradients in forearcs, with an application to Franciscan subduction in California, *J. Geophys. Res.*, *96*, 621–641, 1991.

Dragert, H., R. D. Hyndman, G. C. Rogers, and K. Wang, Current deformation and the width of the seismogenic zone of the northern Cascadia subduction thrust, *J. Geophys. Res.*, *99*, 653–668, 1994.

Gomberg, J., K. Priestley, and J. Brune, The compressional velocity structure of the crust and upper mantle of northern Mexico and the border region, *Bull. Seismol. Soc. Am.*, *79*, 1496–1519, 1989.

Harris, R. N., and K. Wang, Thermal models of the Middle America Trench at the Nicoya Peninsula, Costa Rica, *Geophys. Res. Lett.*, *29*(21), 2010, doi:10.1029/2002GL015406, 2002.

Helsley, C. E., J. B. Nation, and R. P. Meyer, Seismic refraction observations in southern Mexico, *Eos Trans. AGU*, *56*, 452, 1975.

Hutchison, I., The effects of sedimentation and compaction on oceanic heat flow, *Geophys. J. R. Astron. Soc.*, *82*, 439–459, 1985.

Hutton, W., C. DeMets, O. Sanchez, G. Suarez, and J. Stock, Slip kinematics and dynamics during and after the 1995 October 9 M_w = 8.0 Colima-Jalisco earthquake, Mexico, from GPS constraints, *Geophys. J. Int.*, *146*, 637–658, 2001.

Hyndman, R. D., and K. Wang, Thermal constraints on the zone of major thrust earthquake failure: The Cascadia subduction zone, *J. Geophys. Res.*, *98*, 2039–2060, 1993.

Hyndman, R. D., and K. Wang, The rupture zone of Cascadia great earthquakes and the thermal regime, *J. Geophys. Res.*, *100*, 22,133–22,154, 1995.

Hyndman, R. D., K. Wang, and M. Yamano, Thermal constraints on the seismogenic portion of the southwestern Japan subduction thrust, *J. Geophys. Res.*, *100*, 15,373–15,392, 1995.

Hyndman, R. D., M. Yamano, and D. A. Oleskevich, The seismogenic zone of subduction thrust faults, *Island Arc*, *6*, 244–260, 1997.

Kamiya, S., and Y. Kobayashi, Seismological evidence for the existence of serpentinized wedge mantle, *Geophys. Res. Lett.*, *27*, 819–822, 2000.

Klitgord, K., and J. Mammerickx, Northern East Pacific Rise: Magnetic anomaly and bathymetric framework, *J. Geophys. Res.*, *87*, 6725–6750, 1982.

Kostoglodov, V., and W. Bandy, Seismotectonic constraints on the convergence rate between the Rivera and North American plates, *J. Geophys. Res.*, *100*, 17,977–17,989, 1995.

Kostoglodov, V., and J. F. Pacheco, One hundred years of seismicity in Mexico, Inst. de Geofacute;s., Univ. Nac. Autonoma de Mexico, Mexico City, 1999.

Kostoglodov, V., W. Bandy, J. Cominguez, and M. Mena, Gravity and seismicity over the Guerrero seismic gap, Mexico, *Geophys. Res. Lett.*, *23*, 3385–3388, 1996.

Langseth, M. G., and E. A. Silver, The Nicoya convergent margin: A region of exceptionally low heat flow, *Geophys. Res. Lett.*, *23*, 891–894, 1996.

Marone, C., D. M. Saffer, K. M. Frye, and S. Mazzoni, Laboratory results indicating intrinsically stable frictional behaviour of illite clay, *Eos Trans. AGU*, *82*(47), Fall Meet. Suppl., Abstract T51G-06T51G-06, 2001.

Melbourne, T., I. Carmichael, C. DeMets, K. Hudnut, O. Sanchez, J. Stock, G. Suarez, and F. Webb, The geodetic signature of the M8.0 Oct. 9, 1995, Jalisco subduction earthquake, *Geophys. Res. Lett.*, *24*, 6715–6718, 1997.

Mendoza, C., and S. H. Hartzell, Slip distribution of the 19 September 1985 Michoacan, Mexico, earthquake: Near-source and teleseismic constraints, *Bull. Seismol. Soc. Am.*, *79*, 655–669, 1989.

Mendoza, C., and S. Hartzell, Fault-slip distribution of the 1995 Colima-Jalisco, Mexico, earthquake, *Bull. Seismol. Soc. Am.*, *89*, 1338–1344, 1999.

Michaud, F., J. J. Danobeitia, R. Carbonell, R. Bartolome, D. Cordoba, L. Delgado, F. Nunez-Cornu, and T. Monfret, New insights into the subducting oceanic crust in the Middle American Trench of western Mexico (17–19°N), *Tectonophysics*, *318*, 187–200, 2000.

Molnar, P., and P. England, Temperatures, heat flux and frictional stress near major thrust faults, *J. Geophys. Res.*, *95*, 4833–4856, 1990.

Moore, J. C., and D. Saffer, Updip limit of the seismogenic zone beneath the accretionary prism of southwest Japan: An effect of diagenetic to low-grade metamorphic processes and increasing effective stress, *Geology*, *29*, 183–186, 2001.

Moore, J. C., J. S. Watkins, T. H. Shipley, K. J. McMillen, S. B. Bachman, and N. Lundberg, Geology and tectonic evolution of a juvenile accretionary terrane along a truncated convergent margin: Synthesis of results from Leg 66 of the Deep Sea Drilling Project, southern Mexico, *Geol. Soc. Am. Bull.*, *93*, 847–861, 1982.

Nava, F., et al., Structure of the Middle America Trench in Oaxaca, Mexico, *Tectonophysics*, *154*, 241–251, 1988.

Oleskevich, D. A., R. D. Hyndman, and K. Wang, The updip and downdip limits to great subduction earthquakes: Thermal and structural models of Cascadia, south Alaska, SW Japan, and Chile, *J. Geophys. Res.*, *104*, 14,965–14,991, 1999.

Ortiz, M., S. K. Singh, V. Kostoglodov, and J. Pacheco, Source areas of the Acapulco-San Marcos, Mexico earthquakes of 1962 (M 7.1; 7.0) and 1957 (M 7.7), as constrained by tsunami and uplift records, *Geofis. Int.*, *39*, 337–348, 2000a.

Ortiz, M., V. Kostoglodov, S. K. Singh, and J. Pacheco, Jalisco-Colima earthquake (M_w 8) based on the analysis of tsunami records at Manzanillo and Navidad, Mexico, *Geofis. Int.*, *39*, 349–357, 2000b.

Pacheco, J., et al., The October 9, 1995 Colima-Jalisco, Mexico earthquake (M_w 8): An aftershock study and a comparison of this earthquake with those of 1932, *Geophys. Res. Lett.*, *24*, 2223–2226, 1997.

Pardo, M., and G. Suarez, Steep subduction geometry of the Rivera plate beneath the Jalisco block in western Mexico, *Geophys. Res. Lett.*, *20*, 2391–2394, 1993.

Pardo, M., and G. Suarez, Shape of the subducted Rivera and Cocos plates in southern Mexico: Seismic and tectonic implications, *J. Geophys. Res.*, *100*, 12,357–12,373, 1995.

Peacock, S. M., Large-scale hydration of the lithosphere above subducting slabs, *Chem. Geol.*, *108*, 49–59, 1993.

Peacock, S. M., and R. D. Hyndman, Hydrous minerals in the mantle wedge and the maximum depth of subduction thrust earthquakes, *Geophys. Res. Lett.*, *26*, 2517–2520, 1999.

Peacock, S. M., and K. Wang, Seismic consequences of warm versus cool subduction metamorphism: Examples from southwest and northeast Japan, *Science*, *286*, 937–939, 1999.

Prol-Ledesma, R. M., Terrestrial heat flow in Mexico, in *Terrestrial Heat Flow and the Lithosphere Structure*, edited by V. Cermak, and L. Rybach, pp. 475–485, Springer-Verlag, New York, 1991.

Prol-Ledesma, R. M., V. M. Sugrobov, E. L. Flores, G. Juarez, Y. B. Smirnov, A. P. Gorshkov, V. G. Bondarenko, V. A. Rashidov, L. N. Nedopekin, and V. A. Gavrilov, Heat flow variations along the Middle America Trench, *Mar. Geophys. Res.*, *11*, 69–76, 1989.

Reinen, L. A., Seismic and aseismic slip indicators in serpentinite gouge, *Geology*, *28*, 135–138, 2000.

Ruff, L. J., and R. W. Tichelaar, What controls the seismogenic plate interface in subduction zones?, in *Subduction: Top to Bottom*, *Geophys. Monogr. Ser.*, vol. 96, edited by G. E. Bebout, D. W. Scholl, S. H. Kirby, and J. P. Platt, pp. 105–111, AGU, Washington, D. C., 1996.

Scholz, C. H., *The Mechanics of Earthquakes and Faulting*, 439 pp., Cambridge Univ. Press, New York, 1990.

Shephard, L. E., and K. J. McMillen, Sedimentation rates of the southern Mexico continental margin, Deep Sea Drilling Project Leg 66, *Initial Rep. Deep Sea Drill. Proj., 66*, 445–452, 1981.

Singh, S. K., J. Havskov, K. C. McNally, L. Ponce, T. Hearn, and M. Vassiliou, The Oaxaca, Mexico earthquake of 29 November 1978: A preliminary report on aftershocks, *Science*, *207*, 1211–1213, 1980.

Singh, S. K., L. Ponce, and S. P. Nishenko, The great Jalisco, Mexico, earthquake of 1932: Subduction of the Rivera Plate, *Bull. Seismol. Soc. Am.*, *75*, 1301–1313, 1985.

Singh, S. K., et al., The Oaxaca earthquake of 30 September 1999 (M_w = 7.5): A normal-faulting event in the subducted Cocos Plate, *Seismol. Res. Lett.*, *71*, 67–78, 2000.

Smith, D. L., C. E. Nuckels, R. L. Jones, and G. A. Cook, Distribution of heat flow and radioactive heat generation in northern Mexico, *J. Geophys. Res.*, *84*, 2371–2379, 1979.

Stewart, G. S., E. P. Chael, and K. C. McNally, The November 29, 1978, Oaxaca, Mexico, earthquake: A large simple event, *J. Geophys. Res.*, *86*, 5053–5060, 1981.

Stolte, C., K. C. McNally, J. Gonzalez-Ruiz, G. W. Simila, A. Reyes, C. Rebollar, L. Munguia, and L. Mendoza, Fine structure of a post-failure Wadati-Benioff zone, *Geophys. Res. Lett.*, *13*, 577–580, 1986.

Suarez, G., T. Monfret, G. Wittlinger, and C. David, Geometry of subduction and depth of the seismogenic zone in the Guerrero gap, Mexico, *Nature*, *345*, 336–338, 1990.

Suyehiro, K., N. Takahashi, Y. Ariie, Y. Yokoi, R. Hino, M. Shinohara, T. Kanazawa, N. Hirata, H. Tokuyama, and A. Taira, Continental crust, crustal underplating, and low-Q upper mantle beneath an oceanic island arc, *Science*, *272*, 390–392, 1996.

Tichelaar, B. W., and L. J. Ruff, Depth of seismic coupling along subduction zones, *J. Geophys. Res.*, *98*, 2017–2037, 1993.

Tse, S. T., and J. R. Rice, Crustal earthquake instability in relation to the depth variation of frictional slip properties, *J. Geophys. Res.*, *91*, 9452–9472, 1986.

UNAM Seismology Group, The September 1985 Michoacan earthquakes: Aftershock distribution and history of rupture, *Geophys. Res. Lett.*, *13*, 573–576, 1986.

Vacquier, V., J. G. Sclater, and C. E. Corry, Studies of the thermal state of the Earth. The 21st paper: Heat-flow, eastern Pacific, *Bull. Earthquake Res. Inst. Univ. Tokyo*, *45*, 375–393, 1967.

Valdes, C. M., W. D. Mooney, S. K. Singh, R. P. Meyer, C. Lomnitz, J. H. Luetgert, C. E. Helsley, B. T. R. Lewis, and M. Mena, Crustal structure of Oaxaca, Mexico, from seismic refraction measurements, *Bull. Seismol. Soc. Am.*, *76*, 547–563, 1986.

van den Beukel, J., and R. Wortel, Temperatures and shear stresses in the upper part of a subduction zone, *Geophys. Res. Lett.*, *14*, 1057–1060, 1987.

Vrolijk, P., On the mechanical role of smectite in subduction zones, *Geology*, *18*, 703–707, 1990.

Wang, C. Y., Sediment subduction and frictional sliding in a subduction zone, *Geology*, *8*, 530–533, 1980.

Wang, K., and E. E. Davis, Thermal effect of marine sedimentation in hydrothermally active areas, *Geophys. J. Int.*, *110*, 70–78, 1992.

Wang, K., and J. He, Mechanics of low-stress forearcs: Nankai and Cascadia, *J. Geophys. Res.*, *104*, 15,191–15,205, 1999.

Wang, K., R. D. Hyndman, and M. Yamano, Thermal regime of the southwest Japan subduction zone: Effects of age history of the subducting plate, *Tectonophysics*, *248*, 53–69, 1995a.

Wang, K., T. Mulder, G. C. Rogers, and R. D. Hyndman, Case for very low coupling stress on the Cascadia subduction fault, *J. Geophys. Res.*, *100*, 12,907–12,918, 1995b.

Wang, K., R. Wells, S. Mazzotti, R. D. Hyndman, and T. Sagiya, A revised dislocation model of interseismic deformation of the Cascadia subduction zone, *J. Geophys. Res.*, *108*, doi:10.1029/2001JB001227, in press, 2003.

Wessel, P., and W. H. F. Smith, New version of the Generic Mapping Tools released, *Eos Trans. AGU*, *76*, 329, 1995.

Zhang, Z., and S. Y. Schwartz, Depth distribution of moment release in underthrusting earthquakes at subduction zones, *J. Geophys. Res.*, *97*, 537–544, 1992.

Ziagos, J. P., D. D. Blackwell, and F. Mooser, Heat flow in southern Mexico and the thermal effects of subduction, *J. Geophys. Res.*, *90*, 5410–5420, 1985.

C. A. Currie, Pacific Geoscience Centre, Geological Survey of Canada, 9860 West Saanich Road, Sidney, British Columbia, Canada, V8L 4B2. (ccurrie@pgc.nrcan.gc.ca)

R. D. Hyndman and K. Wang, 9860 W Saanich Rd/, POB 6000, Sidney, British Columbia, Canada, V8L 4B2. (hyndman@pgc.nrcan.gc.ca; wang@pgc.nrcan.gc.ca)

V. Kostoglodov, Instituto de Geofisica, Universidad Nacional Autonoma de Mexico, Coyoacan, DF 04510 Mexico City, Mexico. (vladimir@ollin.igeofcu.unam.mx)